Hydrogen Elimination from Ethylene by Laser-Ablated Zr Atoms: An Infrared Spectroscopic Investigation of the Reaction Intermediates in a Solid Argon Matrix

Han-Gook Cho and Lester Andrews*

Department of Chemistry, University of Virginia, P.O. Box 400319, Charlottesville, Virginia 22904-4319

Received: January 30, 2004; In Final Form: February 25, 2004

Intermediates of the hydrogen elimination reaction of ethylene by laser-ablated Zr atoms have been isolated in an argon matrix and investigated by means of infrared spectroscopy. The strong absorptions in the region of 1500−1660 cm^{-1} are due to the Zr−H stretching modes of several intermediates. There are at least three different groups of product absorptions based on the behaviors upon broad-band photolysis and annealing. Among them, the insertion and dihydrido complexes, presumed in previous studies of the hydrogen elimination of ethylene by Zr atoms, are identified. In addition, the remaining Zr−H stretching absorptions, along with absorptions in the C≡C stretching and other regions, suggest that ethynyl zirconium trihydride is also formed in the hydrogen elimination reaction. Formation of this compound is consistent with the fact that C_2H_2 and C_2D_2 as well as CHCD are produced in the reaction of Zr + CH_2CD_2. Density functional theory calculations for the reaction intermediates are also carried out, and the molecular properties and vibrational characteristics are compared with the experimental values.

Introduction

Insertion and rearrangement reactions of transition-metal compounds are considered fundamental steps in various industrially important catalytic processes.[1] Particularly the mechanism of hydrogen elimination from ethylene by ablated transition-metal atoms has recently drawn broad attention.[2−6] Siegbahn, Blomberg, and Svensson theoretically investigated the activation of the C−H bond in ethylene by second-row transition-metal atoms, which eventually lead to hydrogen elimination.[7,8] Their study showed that the transition metal first forms a strongly bound complex with ethylene, which later rearranges to an insertion product. The results indicate that zirconium among the second-row transition metals forms the most stable insertion products with ethylene as well as methane.[7] These workers suggested a reaction path for the H_2 elimination reaction: M + ethylene → π complex → insertion product → dihydrido complex → M−C_2H_2 + H_2.

Reaction-rate coefficients of several hydrocarbons including ethylene with early transition metals and their neutral diatomic oxides were measured by Parnis et al.[6] They concluded that C−H bond insertion followed by the elimination of H_2 is indeed the operative mechanism for the reaction of both metal atoms and metal oxides. The hydrogen elimination reactions of ethylene by early second-row transition metals were later studied in depth by Weisshaar and co-workers.[2−4,9−13] In a series of studies, they investigated the reactivity of ground-state, neutral transition-metal atoms in the left-hand side of the 4d series with alkenes. By use of a fast-flow reactor and a 157-nm photoionization scheme, they identified Zr−$C_2H_4^+$ and Zr−$C_2H_2^+$ [9−11] and explained their results on the basis of the reaction mechanism described above. Davis et al. also studied a hydrogen-elimination reaction by zirconium atoms using a molecular beam apparatus, and their RRKM calculation results indicated that the barrier for C−H insertion is lower than the barrier for association.[5,14]

Weisshar et al. also examined theoretically the structures and energies of the reaction intermediates and transition states and discussed a possible singlet reaction path instead of the conventional triplet reaction path, based upon the feasibilities of the structures of transition states and the presence of an exit channel barrier.[15] The formation of the strongly bound ZrC_2H_4 complex is relatively well understood. Initial formation of the weakly bound π complex of zirconium and ethylene is followed by transformation to a long-lived metallacyclopropane complex, which involves a single CC bond. However, remaining parts of the reaction mechanism, which include the following C−H insertion, hydrogen migration to the dihydrido complex, and elimination of hydrogen, still remain to be examined.

Recently, Manceron et al. reported an infrared matrix isolation study of the initial steps of the thermal ethylene reaction with titanium atoms.[16] They identified two groups of absorption bands based upon the differences in relative intensity increase on electronic excitation of Ti with visible light irradiation. They assigned the two groups of absorption bands to the two oxidative reaction products, the insertion, and a metallic cyclic dihydride species.

The second-row transition metals are known to be more reactive to alkenes in the hydrogen-elimination reaction.[9] Especially the reaction between zirconium and ethylene has been considered as a model system to study the reaction path and intermediates involved.[5,12,14,15] In this study, the reaction of laser-ablated zirconium atoms with ethylene diluted in argon was carried out, and the products captured in the argon matrix were investigated by means of infrared spectroscopy. Results indicate that there are at least three groups of absorption bands, each from a different reaction intermediate, and their vibrational characteristics are compared with the theoretical values.

Experimental and Computational Methods

Laser-ablated zirconium atoms (Johnson-Matthey) were reacted with C_2H_4, C_2D_4, $^{13}C_2H_4$ (Cambridge Isotope Laboratories,

* To whom correspondence may be addressed. E-mail: lsa@virginia.edu.

10.1021/jp049566q CCC: $27.50
Published on Web 04/07/2004

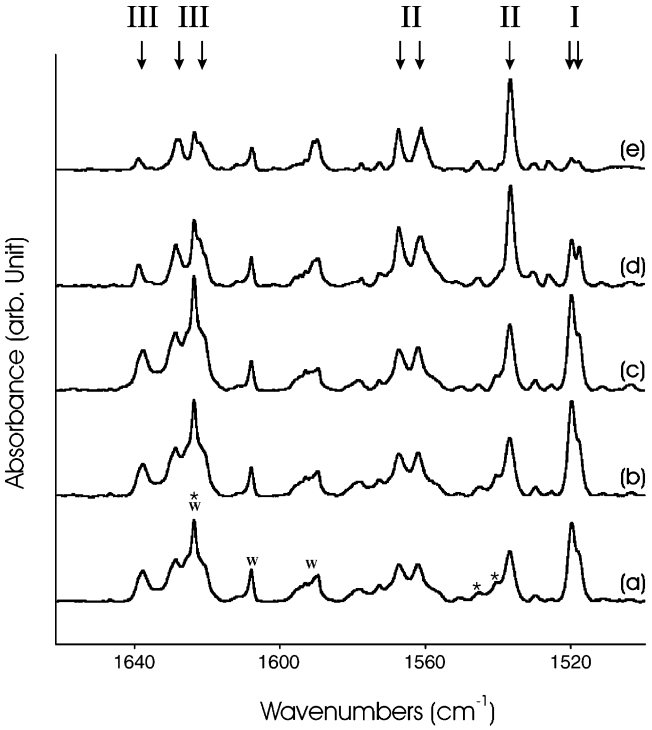

Figure 1. Infrared spectra in the region of 1500−1660 cm^{-1} for laser-ablated Zr atoms co-deposited with Ar/C_2H_4 at 7 K. (a) Zr + 0.5% C_2H_4 in Ar co-deposited for 1 h. (b) After broad-band photolysis with a filter (>530 nm) for 15 min. (c) After broad-band photolysis with a filter (>320 nm) for 15 min. (d) After annealing to 26 K. (e) After annealing to 32 K. I, II, or III stands for the group identification for product band. W and * indicate water impurity and zirconium hydride absorptions.

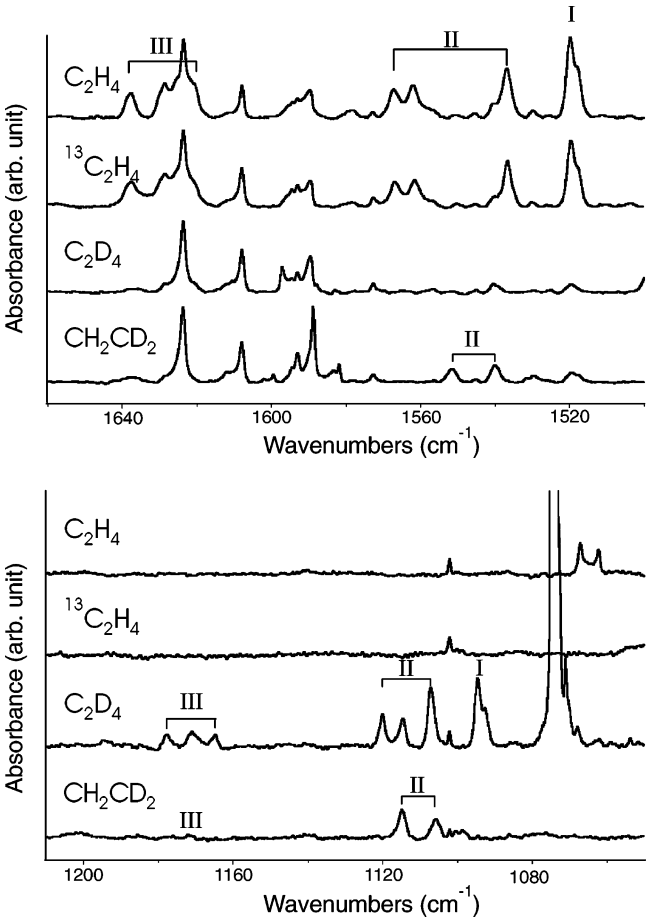

Figure 2. Infrared spectra in the regions of 1500−1660 and 1050−1210 cm^{-1} for laser-ablated Zr atoms co-deposited with ethylene isotopomers diluted in Ar at 7 K. The product absorptions are identified with I, II, or III, depending on the group.

99%), and CH_2CD_2 (MSD Isotopes) in excess argon during condensation at 7 K using a closed-cycle He refrigerator (Air Products HC-2). The methods are previously described in detail elsewhere.[17−20] Concentrations of gas mixtures range between 0.25 and 2% but in most cases are typically 0.5% in argon. After reaction, infrared (IR) spectra were recorded at a resolution of 0.5 cm^{-1} using a Nicolet 550 spectrometer with a HgCdTe detector. Later samples were irradiated by a mercury arc lamp and annealed, and more spectra were recorded.

Complementary density functional theory (DFT) calculations were carried out using the Gaussian 98 package,[21] B3LYP density functional, 6-311+G(2d,p) basis sets for C and H, and LanL2 pseudopotential and LanL2DZ basis for Zr to provide a consistent set of vibrational frequencies for all of the reaction intermediates. Geometries were fully relaxed during optimization, and the optimized geometry was confirmed via vibrational analysis. All the vibrational frequencies were calculated analytically. Zero-point energy is included in calculation of the binding energy of a metal complex.

Results and Discussion

Infrared Spectra. Figure 1 shows IR spectra in the region of 1500−1660 cm^{-1} for laser-ablated Zr atoms co-deposited with Ar/C_2H_4 at 7 K, where strong product absorptions are found at 1518.0, 1519.8, 1536.9, 1561.9, 1567.3, 1620.8, 1628.8, and 1638.6 cm^{-1}. Although ^{13}C substitution leads to negligible shifts in frequencies of the absorptions, deuteration results in large shifts in the frequencies as shown in Figure 2. This indicates that they are in fact all Zr−H stretching bands. In earlier studies, the hydrogen stretching absorptions of zirconium hydrides are also observed in the same frequency region.[22,23]

Irradiation with a broad-band Hg lamp and a filter (>530 nm) leads to increases in all of the absorptions. We find approximately 16% growth for the absorptions at 1518.0 and 1519.8 cm^{-1} (I), 20% growth of the absorptions at 1536.9, 1561.9, and 1567.3 cm^{-1} (II), and 10% growth of the absorptions at 1620.8, 1628.8, and 1638.6 cm^{-1} (III). While following photolysis with other filters (λ > 480, >420, and >380 nm) did not cause any noticeable change in the spectrum, photolysis with a filter transmitting an even shorter wavelength (λ > 320 nm) results in an additional 17% increase in intensity of the absorptions at 1536.9, 1561.9, and 1563.7 cm^{-1} and 12% increases in intensity of the absorptions at 1620.8, 1628.8, and 1638.6 cm^{-1}, while the other product absorptions at 1518.0 and 1519.8 cm^{-1} remain almost unchanged.

Figure 1 also shows changes in the spectrum upon annealing. The absorption at 1519.8 cm^{-1} decrease markedly on annealing and the neighboring absorption at 1518.0 cm^{-1} follows this trend, while the absorptions at 1536.9, 1561.9, and 1567.3 cm^{-1} (II) grow continuously up to 26 K. On the other hand, the absorptions at 1620.8, 1628.8, and 1638.6 cm^{-1} (III) decrease gradually in the course of annealing. Because of the growth on both photolysis and annealing, the absorptions at 1536.9, 1561.9, and 1567.3 cm^{-1} (II) eventually end up with about 90% increases in intensity.

Not only the absorptions shown in Figure 1, but all the observed product bands in this study as well, can be sorted into three groups based upon their behavior on photolysis and annealing, and calculations: each group is believed to arise from a different reaction product. Figures 1−4 show the product

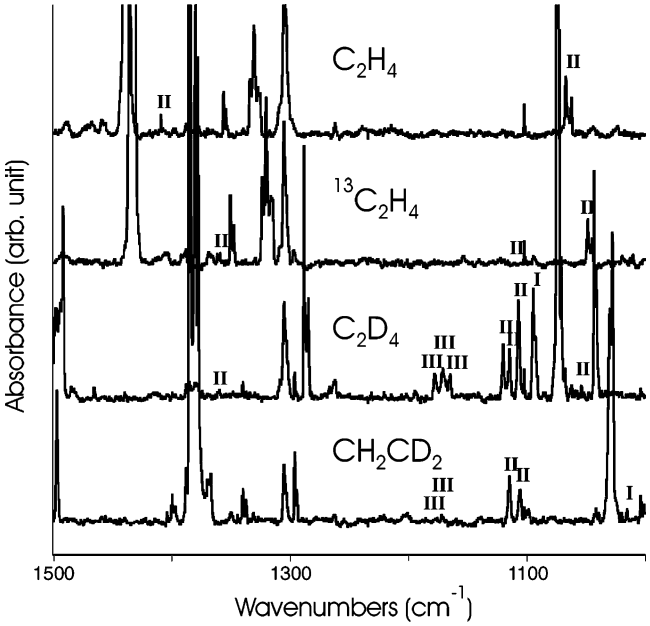

Figure 3. Infrared spectra in the region of 1000−1500 cm^{-1} for laser-ablated Zr atoms co-deposited with ethylene isotopomers diluted in Ar at 7 K. I, II, or III indicates the group for the product band.

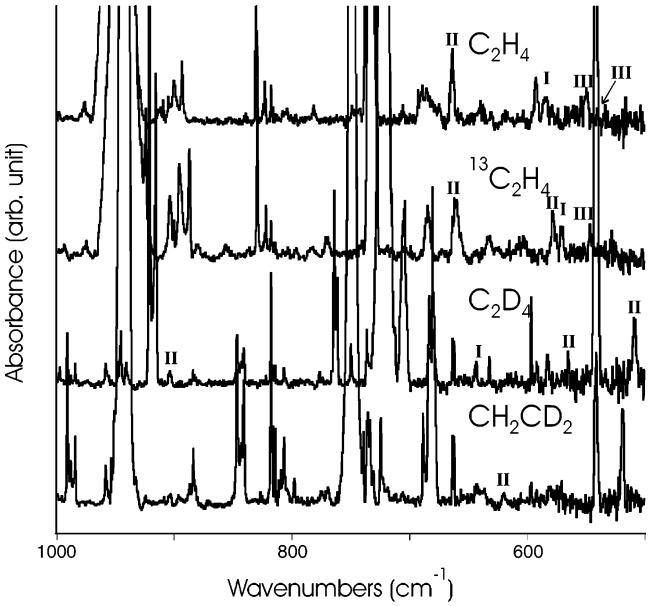

Figure 4. Infrared spectra in the region of 500−1000 cm^{-1} for laser-ablated Zr atoms co-deposited with ethylene isotopomers diluted in Ar at 7 K. I, II, or III indicates the group for the product band.

absorptions marked with I, II, and III, depending on the group identification. The absorptions of group I increase on photolysis, particularly on irradiation of light with a wavelength longer than 530 nm; however, they decrease on annealing and almost disappear at 32 K. The absorptions of group II grow most on photolysis with light not only longer than 530 nm but 320−380 nm as well. They are the only group of absorptions that increase on annealing up to 26 K. The absorptions of group III grow slightly on photolysis with light of wavelength 320−380 nm as well as longer than 530 nm and decrease gradually on annealing.

The product bands observed for the Zr + ethylene reaction are listed in three groups in Table 1. It is notable that the strongest absorptions of the three groups originate mostly from the Zr−H stretching modes. Because of the heavy zirconium atom, the Zr−H stretching mode is effectively decoupled from other vibrational modes of the complex, and the pattern of the absorptions can give valuable structural information. The two Zr−H absorptions less than 2 cm^{-1} apart of group I (Figure 1) indicate that there may be only one hydrogen atom bonded to the Zr atom, whereas those about 20 cm^{-1} or more apart for groups II and III suggest that the metal atom of the reaction product has at least two metal−hydrogen bonds.

Group I. A relatively small number of absorptions are assigned to group I as listed in Table 1. The absorptions at 1518.0 and 1519.8 cm^{-1} shown in Figure 1, the lowest Zr−H stretching frequencies, are overlapped and also show similar behavior on photolysis and annealing regardless of isotopomer. The absorptions are attributed to the same hydrogen stretching mode arising from two different sites in the matrix.

On photolysis, the absorptions of group I strengthen along with other product absorptions. It is notable at this point that no product absorptions observed in this study decrease on photolysis. This suggests that the electronically excited Zr atom either reacts with nearby ethylene molecule or transforms metal-bound complexes that do not have noticeable absorption to the reaction products responsible for the observed absorptions. On the other hand, marked decrease of the absorptions in group I on annealing as shown in Figure 1 indicates that they originate from a relatively unstable reaction product so that thermal energy eventually transforms the product to more stable ones.

Group II. More absorptions belong to this group. An increase of the absorptions of group II on both photolysis and annealing indicates that the absorptions probably arise from a relatively stable reaction product. The strong Zr−H absorptions of group II are highly visible. The absorption at 1536.9 cm^{-1} and the two absorptions at 1567.3 and 1561.9 cm^{-1} probably arise from different Zr−H stretching modes of the complex.

Shown in Figure 3 is IR spectra in the region of 1000−1500 cm^{-1} for laser-ablated Zr atoms co-deposited with ethylene isotopomers diluted in Ar at 7 K. The absorption at 1409.6 cm^{-1} shows isotope shifts of −47.7 and −47.2 cm^{-1} on ^{13}C and D substitutions. The band is attributed to a C−C stretching mode of a strongly bound metal−ethylene complex. Formation of metal−carbon σ bonds considerably weakens the C═C bond of ethylene, resulting in a lower frequency. The C−C stretching mode in the metal-bound complex also causes a change in the Zr−C distance, which is accompanied by a dipole moment change and produces IR activity.

The strong absorptions at 1067.1 and 1062.2 cm^{-1} show isotopic shifts of −19 and −161 cm^{-1} on ^{13}C and D substitutions and $^{12}C/^{13}C$ and H/D isotopic ratios of 1.018 and 1.178. Most likely, the band arises from a CCH bending mode. Another band observed at 664 cm^{-1} in Figure 4 gives a minimal ^{13}C isotopic shift of −4 cm^{-1} but a sizable D isotopic shift of −99 cm^{-1}. The absorptions presumably originate from a bending mode consisting almost exclusively of displacements of Zr and H atoms, such as the ZrH_2 scissoring.

Group III. Figure 5 shows product absorptions at 1959.8, 1960.9, and 1962.7 cm^{-1} in the spectrum of Zr + C_2H_4, and similar absorptions are also found in the spectra of the isotopomers. The weaker absorptions of acetylene clusters are also noticeable on the red-side edge of the absorptions. The isotopic shifts by ^{13}C and D substitution are −70 and −113 cm^{-1}, and $^{12}C/^{13}C$ and H/D isotopic ratios are 1.037 and 1.061. On the basis of the frequencies and isotopic shifts, the bands most probably arise from the C≡C stretching mode. Acetylene is the final product of the hydrogen-elimination reaction of ethylene. However, its π complex should lead to a significantly

TABLE 1: Frequencies (cm^{-1}) of Observed Product Absorptions

group	C_2H_4	C_2D_4	$^{13}C_2H_4$	CH_2CD_2
I		1419.3	1549.7	
	1519.8, 1518.0	1094.6, 1092.6	1519.5, 1517.9	1404.3, 1015.2
				924.8
		643		
	584		570	
II	1567.3, 1561.9	1120.1, 1114.6	1566.8, 1561.5	1551.6, 1539.8
	1536.9	1107.1	1536.6	1114.7, 1105.7
	1409.6	1361.4	1361.9	
	1067.1, 1062.2	903.5	1048.4, 1044.8	
		582.7		
	664	565	660	619
	592	509	578	
III	1962.7, 1960.9, 1959.8	1849.7, 1847.8, 1846.8	1892.6, 1890.8, 1889.9	1962.4, 1960.8, 1959.6, 1849.5, 1848.1, 1847.3
	1638.6	1177.7	1638.6	1171
	1628.8, 1620.8	1171.0, 1164.8	1628.6, 1620.8	1611.9, 1599.4
				1176.6, 1171.2
	555			
	549		547	

lower frequency, due to the weakened C≡C bond, and a much weaker absorption. The C≡C stretching band, which for acetylene is infrared inactive, becomes strong only when the triple bond is highly polarized by a strong electron-donating or -withdrawing group. Therefore, the absorptions probably arise from a CCH moiety bonded to a metal atom along the axis of the C≡C bond.

The strong Zr−H stretching absorptions of group III are observed at 1620.8, 1628.8, and 1638.6 cm^{-1} in Figure 1. The absorptions at 1620.8 and 1628.8 cm^{-1} are partly overlapped with the absorption of water residue at 1623.5 cm^{-1}. Earlier studies have shown that the Zr−H stretching frequency of zirconium hydrides generally increase with the Zr valence bonds, and the frequency of the Zr−H stretch of ZrH_4 is in fact observed at 1623.6 cm^{-1}. On the basis of the high frequencies of Zr−H stretch absorptions of group III, much higher than those of groups I and II, the Zr−H stretching absorptions suggest that three hydrogen atoms are presumably bonded to the Zr atom in the reaction product, while the Zr atom is bonded to an ethynyl moiety. The most probable product that would be energetically favorable and also fit to the characteristics of interacting C≡C and Zr−H stretching absorptions is ethynyl zirconium trihydride, which will be discussed below.

Other Products. The strong bending-mode absorptions of acetylene shown in Figure 6 confirm the formation of acetylene, the final reaction product of the hydrogen-elimination reaction.

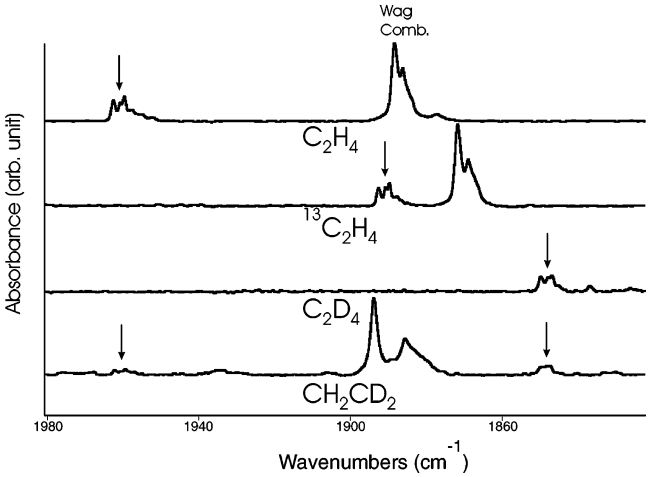

Figure 5. Infrared spectra in the C≡C stretching region for laser-ablated Zr atoms co-deposited with ethylene isotopomers diluted in Ar at 7 K. An arrow indicates the product absorption.

On the basis of the intensities of the hydrogen stretch bands of acetylene and ethylene in the region of 2800−3400 cm^{-1}, we estimate that typically about 20% of the ethylene precursor is converted to acetylene and hydrogen in the present experiment. Figure 6 also shows that not only CHCD but CHCH and CDCD as well are generated from CH_2CD_2. It should be noted that formation of C_2H_2 and C_2D_2 is precluded if the hydrogen elimination follows the reaction path proposed in previous studies.[5,14,15] The estimated concentration ratio of C_2H_2, CHCD, and C_2D_2 by comparing the measured and calculated intensities of the bending-mode band of the isotopomers is approximately 1:6:2.

Because of the hydrogen generated in the reaction chamber by laser-ablated metal atoms, isolated zirconium hydrides are also formed, and some of the Zr−H stretching bands are identified. The bands at 1540.8 and 1545.3 cm^{-1} (labeled ∗) in Figure 1 are in fact ZrH and ZrH_3 absorptions, and the ZrH_4 absorption at 1623.6 cm^{-1} is believed to be overlapped by a stronger water absorption.[22,23] However, absorptions of the zirconium hydrides are much weaker in the spectra than the Zr−H stretching bands of the Zr−ethylene complexes as shown in Figure 1.

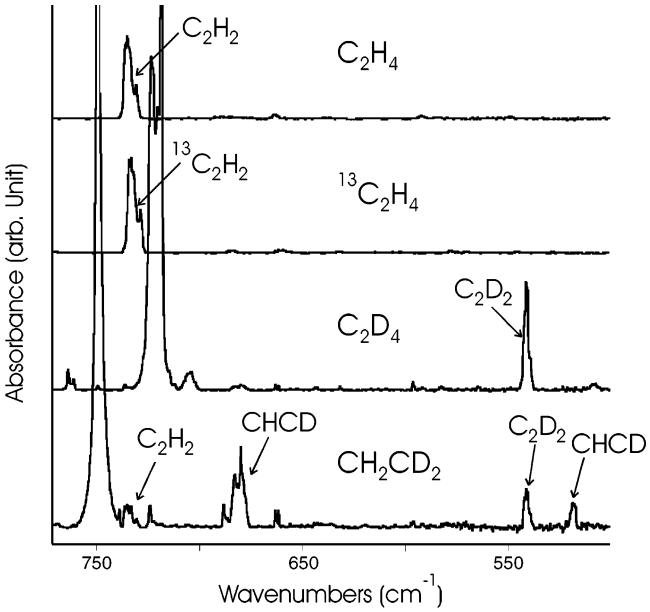

Figure 6. Infrared spectra in the region of 500−800 cm^{-1} for laser-ablated Zr atoms co-deposited with ethylene isotopomers diluted in Ar at 7 K. The acetylene Π_u absorptions are indicated.

TABLE 2: Geometrical Parameters and Physical Constants Calculated (B3LYP/6-311+G(2d, p)/LANL2DZ) for Intermediates in the Hydrogen-Elimination Reaction of Ethylene[a]

parameters	$Zr-C_2H_4$	$ZrH-CHCH_2$	$ZrH_2-C_2H_2$	ZrH_3-CCH
r(C−C)	1.475	1.340	1.331	1.216
r(C−H)	1.088	1.085, 1.088 1.108	1.085, 1.087	1.066
r(C−Zr)	2.184	2.161	2.103, 2.130	2.176
r(Zr−H)		1.879	1.869	1.838
∠CCH	118.5	120.3	130.2, 134.0	180.0
∠HCH	112.7	111.0		
∠CZrC	37.5		36.6	
∠CZrH		127.4	113.7	110.5
∠HZrH			118.8	108.4
q(C)[b,c]	−0.50	−0.71, 0.01	−0.41, −0.30	−0.66, −0.07
q(H)[b,c]	0.12	−0.26, 0.08	−0.26, −0.26	−0.25, −0.25
		0.10, 0.08	0.08, 0.08	−0.25, 0.16
q(Zr)[b]	0.52	0.71	1.08	1.34
μ[d]	1.18	2.79	3.23	1.22
$^1\Delta E$[e]	30.47 ($^1A_1$)	26.07 (^1A)	47.43 ($^1A'$)	37.18 ($^1A_1$)
$^3\Delta E$[e]	28.60 ($^3B_1$)	32.89 ($^3A''$)	36.65 (^3B)	[f]

[a] Bond lengths and angles are in Å and degrees. [b] Mulliken atomic charge. [c] The first value is for the atom closest to the Zr atom. [d] Molecular dipole moment in D. [e] Binding energy in kcal/mol relative to $Zr + C_2H_4$. [f] Attempt to find an optimized structure in the triplet state ends with the structure of the dihydrido complex ($ZrH_2-C_2H_2$).

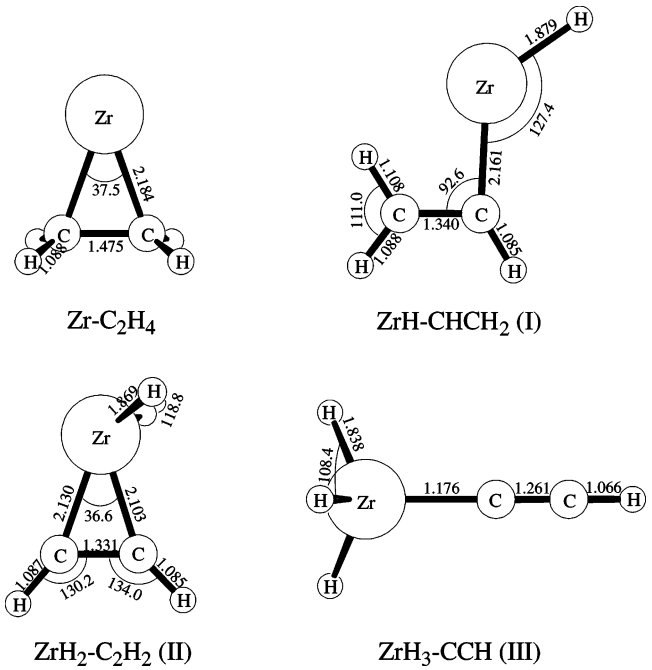

Figure 7. The optimized molecular structures for the reaction intermediates in the infrared ground electronic states. The bond lengths and angles are in Å and degrees.

Calculations. Calculations have been carried out at the B3LYP/6-311+G(2d,p) level for the metallacyclopropane $Zr-C_2H_4$, the insertion product $CH_2CH-Zr-H$, the dihydrido complex $ZrH_2-C_2H_2$, ethynyl zirconium trihydride ZrH_3-CCH, and other related compounds. The geometrical parameters and molecular constants of the reaction intermediates are summarized in Table 2, and the optimized molecular structures are shown in Figure 7. The calculated frequencies are listed along with the experimental values in Tables 3−6.

The optimized molecular structures and other molecular properties including the frequencies for the metallacyclopropane, insertion product, and dihydrido complex are basically consistent with the previous results by Weisshaar et al.[15] One discrepancy found is the most stable triplet state of zirconium metallacyclopropane complex $Zr-C_2H_4$ ($^3B_1$), compared to $^3A_2$ in their study, while the optimized structures are still essentially the same. Calculation results in this study show that a singlet state

TABLE 3: Calculated Vibrational Fundamentals of the Metallacyclopropane Complex[a]

	$Zr-C_2H_4$		$Zr-C_2D_4$		$Zr-^{13}C_2H_4$		Zr−CHCD	
description	freq	int	freq	int	freq	int	freq	int
ν_1 A_1 CH_2 str	3075	1	2239	3	3069	1	3072	1
ν_2 A_1 C═C str	1426	1	1153	16	1418	0	1418	2
ν_3 A_1 CH_2 scis	1065	32	897	12	1036	30	954	12
ν_4 A_1 CH_2 rock	830	0	631	1	824	0	696	1
ν_5 A_1 ZrC_2 str	451	4	431	3	439	4	428	9
ν_6 A_2 CH_2 str	3132	0	2319	0	3120	0	2333	0
ν_7 A_2 CH_2 rock	1192	0	932	0	1180	0	1091	0
ν_8 A_2 CH_2 twist	4667	0	340	0	465	0	348	0
ν_9 B_1 CH_2 str	3148	1	2336	1	3136	1	3140	1
ν_{10} B_1 CH_2 rock	755	0	538	0	754	0	619	0
ν_{11} B_1 ZrCH bend	484	0	357	0	483	0	476	0
ν_{12} B_2 CH_2 str	3067	1	2220	0	3063	1	2229	2
ν_{13} B_2 CH_2 scis	1409	3	1038	3	1404	3	954	12
ν_{14} B_2 CH_2 wag	918	4	779	0	904	5	884	4
ν_{15} B_2 ZrC_2 str	489	21	422	17	476	20	464	13

[a] Frequencies and intensities are in cm^{-1} and km/mol.

($^1A_1$) is the ground state for the metallacyclopropane complex, while a triplet state ($^3A''$) is the ground state for the insertion complex. On the other hand, singlet states, which are favored in formation of more Zr bonds, are the ground states for the dihydrido complex and ethynyl zirconium trihydride.

Earlier studies reported that the early transition metals form a metallacyclopropane, whereas the late ones mostly form a π complex.[7,8] The metallacyclopropane complex differs from the π complex by having a bond between the carbon and metal atoms that is so strong that the bond between the carbon atoms is weakened to a single bond. Formation of the complex is often described by the simple Dewar−Chatt−Cuncanson model.[24,25] Ethylene donates π electron density to an empty σ orbital of the metal, which in turn weakens the π bond of ethylene. This eventually lowers the energy of the π^* orbital so that electrons will be accepted from a back-donating d orbital of the metal atom, forming a strongly bound metal complex.

It is generally accepted that the metallacyclopropane complex converts to the insertion complex along the reaction path of hydrogen elimination. The energy barrier to CH activation for formation of the insertion complex is generally considered the highest one, and no barriers lie above the reactant asymptote all the way to H_2 elemination.[15] The insertion complex has a planar structure at its triplet ground state. While the length of

TABLE 4: Observed and Calculated Frequencies of the Fundamental Bands of the Insertion Complex[a]

										CH_2CD_2					
	C_2H_4			C_2D_4			$^{13}C_2H_4$			$CD_2CH-Zr-H$			$CH_2CD-Zr-D$		
description	exp	calc	int	exp	calc	int	exp	calc	int	exp	calc	int	exp	calc	int
ν_1 A′ CH str		3158	4		2341	0.		3147	4		3122	11		2305	3
ν_2 A′ CH_2 str		3116	12		2298	6		3107	14		2290	15		3097	32
ν_3 A′ CH_2 str		2896	39		2119	21		2888	39		2129	18		2907	46
ν_4 A′ C═C str		1610	3	1419	1464	7	1550	1588	13		1507	2		1606	5
ν_5 A′ ZrH str	1520	1567	526	1095	1114	268	1519	1567	518	1404	1446	539	1015	1028	278
ν_6 A′ CH_2 scis		1405	30		1084	19		1369	26		1168	27		1417	17
ν_7 A′ CH_2 scis		1220	20		1008	7		1203	21		1081	13		1145	3
ν_8 A′ CH_2 rock		899	27	643	652	14		897	26		785	22		751	12
ν_9 A′ CZr str	584	574	58		510	37	570	561	59		492	80		482	68
ν_{10} A′ CZrH IP bend		384	48		296	17		381	48		307	71		239	22
ν_{11} A′ CCZr IP bend		237	41		204	37		231	39		171	34		175	46
ν_{12} A″ CH_2 twist		966	6		764	0.		991	7		963	5		875	0
ν_{13} A″ CH_2 wag		901	28		697	20		892	27		758	9	924.8	949	15
ν_{14} A″ CCZr OOP bend		428	38		317	21		427	37		276	29		328	31
ν_{15} A“ CZrH OOP bend		168	22		125	10		168	22		113	53		83	23

[a] Frequencies and intensities are in cm^{-1} and km/mol. Intensities are all calculated values.

TABLE 5: Observed and Calculated Frequencies of the Fundamental Bands of the Dihydrido Complex[a]

	$ZrH_2-C_2H_2$			$ZrD_2-C_2D_2$			$ZrH_2-^{13}C_2H_2$			ZrHD-C_2HD		
description	exp	calc	int	exp	calc	int	exp	calc	int	exp	calc	int
ν_1 A′ CH str (s)		3168	4		2367	0		3156	4		2348	2
ν_2 A′ CH str (a)		3129	9		2302	2		3119	9		3134	8
ν_3 A′ ZrH_2 s str	1567	1623	299	1120	1150	167	1567	1622	305	1552	1605	437
ν_4 A′ CC str	1410	1469	34	1361	1416	12	1362	1416	27		1441	23
ν_5 A′ CCH IP a bend	1067	1092	84	904	930	32	1048	1074	86		1039	70
ν_6 A′ CCH IP s bend		823	19	583	599	16		822	20		694	19
ν_7 A′ ZrH_2 scis	664	687	165	565	577	62	660	684	162	619	633	121
ν_8 A′ ZrC_2 a str	592	586	85	509	501	85	578	571	82		541	45
ν_9 A′ ZrC_2 s str		553	5		454	16		539	6		518	40
ν_{10} A′ ZrH_2 wag		293	236		211	122		292	234		225	99
ν_{11} A″ ZrH_2 a str	1537	1588	585	1107	1134	307	1537	1588	595	1115	1143	245
ν_{12} A″ CCH a OOP		946	10		754	1		936	1		877.	11
ν_{13} A″ CCH s OOP		681	40		522	21		677	40		570	22
ν_{14} A″ ZrH_2 rock		438	20		315	10		437	20		368	41
ν_{15} A″ ZrH_2 twist		307	58		235	27		305	59		229	96

[a] Frequencies and intensities are in cm^{-1} and km/mol. Intensities are all calculated values.

TABLE 6: Observed and Calculated Frequencies of the Fundamental Bands of Ethynyl Zirconium Trihydride[a]

										CH_2CD_2					
	ZrH_3-CCH			ZrD_3-CCD			$ZrH_3-^{13}C^{13}CH$			ZrH_2D-CCD			$ZrHD_2-CCH$		
description	exp	calc	int	exp	calc	int	exp	calc	int	exp	calc	int	exp	calc	int
ν_1 A_1 C−H str	1963	3432	30	1850	2652	13	1893	3414	33	1849	2652	13	1962	3432	30
ν_2 A_1 CC str	1961	1848	1891	1848	1961										
ν_3 A_1 ZrH_3 s str	1639	1722	249	1178	1221	127	1639	1722	251		1707	323	1171	1211	175
ν_4 A_1 ZrH_3 s def	549	576	292		466	206	547	575	285		525	232		528	173
ν_5 A_1 C−Zr str		430	27		373	10		418	29		419	23		383	19
ν_6 E ZrH_3 a str	1629	1674	947	1171	1193	496	1629	1674	947	1599 1171	1675 1202	470 219	1612 1177	1691 1211	388 252
ν_7 E CCH bend		707	79		560	31		700	80		560 559	18 11		707 707	40 39
ν_8 E ZrH_3 a def	555	599	132		426	60		599	133		592 526	127 18		523 454	76 83
ν_9 E ZrH_3 rock		374	158		287	107		372	154		349 309	862 46		309 300	64 46
ν_{10} E CCZr bend		140	8		123	5		136	8		131 126	4 3		136 132	3 3

[a] Frequencies and intensities are in cm^{-1} and km/mol. Intensities are all calculated values.

the Zr−C bond is slightly shorter than those of the metallacyclopropane complex, the length of the CC bond 1.34 Å is close to that of a CC double bond.

Conversion to the insertion complex from the metallacyclopropane leads to a large increase in infrared absorption. Particularly the absorption intensity of the Zr−H stretch is dramatically higher than those of the vibrational modes of the metallacyclopropane as shown in Table 3; therefore, existence of the reaction intermediate can be identified by the absorption in its infrared spectrum even at a very low concentration. In

comparison with the Zr−H stretch, other vibrational modes of the insertion complex have much lower absorption intensities as listed in Table 4; it is probably the reason not many absorptions of group I, other than the Zr−H bands, are observed.

The dihydrido complex has a C_s structure as shown in Figure 7, compared to the C_2 structure of the triplet state (^{3}B).[15] While the Zr−H bonds are slightly longer in comparison with those of the insertion complex, the CC bond is shorter. Calculation results indicate that the dihydrido complex is the most stable reaction intermediate among the reaction intermediates examined in this study. Previous reaction dynamics studies assume that the detachment of hydrogen occurs from the complex.[5,12,14,15] It should also be noted that many vibrational modes of the dihydrido complex, including the Zr−H and C−H stretches, have exceptionally high absorption intensities as shown in Table 5. Therefore, it is expected that a variation in concentration of the dihydrido complex, during annealing or photolysis, can be monitored with the absorptions.

The optimized geometry of ethynyl zirconium trihydride in its ground state is also shown in Figure 7. Ethynyl zirconium trihydride has never been discussed as a possible reaction product of the Zr + ethylene reaction in previous studies. The molecular energy, however, turned out to be comparable to those of the metallacyclopropane and the insertion complexes.

Assignments. On the basis of the vibrational characteristics and behavior on photolysis and annealing and calculation results, group I is assigned to the insertion complex, and the absorptions are listed in Table 4. A relatively small number of bands are identified for each isotopomer probably because the vibrational modes, other than the Zr−H stretch, do not have high absorption intensities as shown in Table 4.

Group II is believed to arise from the dihydrido complex. The largest growth ratio in intensity on photolysis and the growth on annealing unlike the absorptions in the other two groups indicate that the absorptions originate from the most stable intermediate. Moreover, the vibrational characteristics of the Zr−H and CC stretching modes and ZrH_2 scissoring modes summarized in Table 5 all indicate that they arise from the dihydrido complex.

Group III is attributed to ethynyl zirconium trihydride. The vibrational characteristics of the absorptions in the C≡C stretching region near 1960 cm^{-1}, and the strong Zr−H stretching absorptions point to an acetylene moiety bonded to a metal atom along the C≡C bond axis, and at the same time, three hydrogen atoms are bonded to the metal atom. The observed vibrational characteristics of group III are compared with the calculated values in Table 6. The isotopomers show very good agreement between the observed and calculated values. Calculations were also carried out for other plausible products for the current experimental setup, such as ethynyl zirconium mono hydride and dihydride; however, their vibrational characteristics did not match the observed values.

By comparing the observed integrated intensities of the Zr−H stretching absorptions of the Zr complexes and the C−H stretching absorptions of ethylene with the calculated IR intensities, it is estimated that 0.94, 0.55, and 0.65% of the ethylene precursor are converted to the insertion, dihydrido, and ethynyl trihydride complexes during condensation in our argon matrix experiment. The portion of the dihydrido complex later increases to about 1% after photolysis ($\lambda > 530$ and 380 nm $> \lambda > 320$ nm) and annealing to 26 K. In marked contrast, about 20% of ethylene is transformed into the final product acetylene and the Zr complexes are most probably intermediates in the H_2-elimination reaction.

As described above, C_2H_2 and C_2D_2 are also formed along with CHCD in the reaction of Zr and CH_2CD_2. This cannot occur if hydrogen is released from the dihydrido complex because the hydrogen atoms bonded to the metal atom in the complex are abstracted, one from each carbon atom. However, a fast equilibrium between I ↔ II can also scramble the hydrogen atoms. On the other hand, a different reaction path can be proposed: The insertion or dihydrido complex transforms to ethynyl zirconium trihydride, and hydrogen is later detached from ethynyl zirconium trihydride. In the Zr + CH_2CD_2 reaction case, HC≡C−$ZrHD_2$ and DC≡C−ZrH_2D will be formed as the intermediates, and considering only statistics, C_2H_2, CHCD, and C_2D_2 will be produced with a molar ratio of 1:4:1. The observed molar ratio of 1:6:2 may result with an isotope effect of hydrogen-releasing rates being in the order of H_2, HD, and D_2.

In previous reaction dynamics work, including fast-flow reaction and molecular-beam studies, the metal atoms were thermalized, due to collisions with noble gas molecules, before introduction into the reaction area.[5,9,11−14] On the other hand, in the present reaction setup, ethylene molecules in excess argon react during condensation with the laser-ablated metal atoms, which are generally considered to have higher kinetic and possibly electronic energies. Therefore, it should also be considered that, in the present experiment, there is a possibility of the H_2-elimination reaction following a different reaction path or even of more than one reaction paths.

None of the characteristics of the three groups of absorptions match with those of the zirconium metallacyclopropane complex Zr−C_2H_4. In this study, no band from the metallacyclopropane complex has been identified, probably because the vibrational bands are mostly very weak, as shown in Table 3. As a result, conversion from the metallacyclopropane complex to the insertion product, the dihydrido complex, or ethynyl zirconium trihydride should result in increases in intensity of the corresponding absorptions without noticeable decreases in intensity of any absorptions.

Similarly, no absorptions from Zr−C_2H_2, whose cation is detected in previous reaction dynamics studies,[9−11] are identified in the present work. Experiments in progress with Zr and C_2H_2 reveal new products at 597.1, 1053.9, 1427.8, and 1534.7 cm^{-1}, which are not observed in our C_2H_4 experiments.[26] Calculations show that the IR absorptions of the metal-bound complex are very weak, which might be one of the reasons for nonobservation in the IR spectrum.

Conclusions

Intermediates in the H_2-elimination reaction of ethylene by Zr assumed in previous studies, the insertion and dihydrido complexes, have been identified in our argon matrix investigation. The strong absorptions in the region of 1500−1660 cm^{-1} are assigned to the Zr−H stretching modes of the reaction intermediates and the absorptions at about 1960 cm^{-1} to the C≡C stretching modes. The observed absorptions arising from the reaction intermediates all increase on photolysis, but the growth ratios and the effective wavelengths differ. On the basis of the behaviors on photolysis and annealing, the observed absorptions of the reaction intermediates are sorted into groups for three important reaction intermediates.

Absorptions that increase most on irradiation and show continuous growth on annealing arise from the most stable intermediate, the dihydrido complex. In contrast, bands for the insertion complex are most sensitive to annealing. On the basis of the vibrational characteristics and other properties, ethynyl zirconium trihydride is identified here for the first time. The

compound has comparable molecular energy to those of the metallacyclopropane and insertion complexes. The presence of ethynyl zirconium trihydride among the reaction intermediates also explains the formation of C_2H_2 and C_2D_2 as well as CHCD in the reaction of Zr and CH_2CD_2.

Acknowledgment. We gratefully acknowledge financial support for this work from a N.S.F. Grant CHE 00-78836 and sabbatical leave support (H.-G. Cho) from the Korea Research Foundation (KRF-2003-013-C00044).

References and Notes

(1) Hyla-Kryspin, I.; Niu, S.; Gleiter, R. *Oranometallics* **1995**, *14*, 964.
(2) Yi, S. S.; Blomberg, M. R. A.; Siegbahn, P. E. M.; Weisshaar, J. C. *J. Phys. Chem. A* **1998**, 102.
(3) Blomberg, M. R. A.; Siegbahn, P. E. M.; Yi, S. S.; Noll, R. J.; Weisshaar, J. C. *J. Phys. Chem. A* **1999**, *103*, 7254.
(4) Jiao, C. Q.; Freiser, B. S. *J. Phys. Chem*. **1995**, *99*, 3969.
(5) Stauffer, H. U.; Hinrichs, R. Z.; Schroden, J. J.; Davis, H. F. *J. Phys. Chem. A* **2000**, *104*, 1107.
(6) Parnis, J. M. P.; Lafleur, R. D.; Rayner, D. M. *J. Phys. Chem*. **1995**, *99*, 673.
(7) Siegbahn, P. E. M.; Blomberg, M. R. A.; Svensson, M. *J. Am. Chem. Soc*. **1993**, *115*, 1952.
(8) Blomberg, M. R. A.; Siegbahn, P. E. M.; Svensson, M. *J. Phys. Chem*. **1992**, *96*, 9794.
(9) Carroll, J. J.; Haug, K. L.; Weisshaar, J. C.; Blomberg, M. R. A.; Siegbahn, P. E. M.; Svensson, M. *J. Phys. Chem*. **1995**, *99*, 13955.
(10) Reichert, E. L.; Yi, S. S.; Weisshaar, J. C. *Int. J. Mass Spectrom*. **2000**, *196*, 55.
(11) Wen, Y.; Poremski, M.; Ferrett, T. A.; Weisshaar, J. C. *J. Phys. Chem. A* **1998**, *102*, 8362.
(12) Poremski, M.; Weisshaar, J. C. *J. Phys. Chem. A* **2000**, *104*, 1524.
(13) Carroll, J. J.; Haug, K. L.; Weisshaar, J. C. *J Am. Chem. Soc*. **1993**, *115*, 6962.
(14) Willis, P. A.; Stauffer, H. U.; Hinrichs, R. Z.; Davis, H. F. *J. Phys. Chem. A* **1999**, *103*, 3706.
(15) Poremski, M.; Weissharr, J. C. *J. Phys. Chem. A* **2001**, *105*, 4851.
(16) Lee, Y. K.; Manceron, L.; Papai, I. *J. Phys. Chem. A* **1997**, *101*, 9650.
(17) Chertihin, G. V.; Andrews, L.; Rosi, M.; Bauschlicher, C. W., Jr. *J. Phys. Chem. A* **1997**, *101*, 9085.
(18) Andrews, L.; Zhou, M.; Chertihin, G. V.; Bauschlicher, C. W., Jr. *J. Phys. Chem. A* **1999**, *103*, 6525.
(19) Burkholder, T. R.; Andrews, L. *J. Chem. Phys*. **1991**, *95*, 8697.
(20) Hassanzadeh, P.; Andrews, L. *J. Phys. Chem*. **1992**, *96*, 9177.
(21) Frisch, M. J.; Trucks, G. W.; Schlegel, H. B.; Scuseria, G. E.; Robb, M. A.; Cheeseman, J. R.; Zakrzewski, V. G.; Montgomery, J. A., Jr.; Stratmann, R. E.; Burant, J. C.; Dapprich, S.; Millam, J. M.; Daniels, A. D.; Kudin, K. N.; Strain, M. C.; Farkas, O.; Tomasi, J.; Barone, V.; Cossi, M.; Cammi, R.; Mennucci, B.; Pomelli, C.; Adamo, C.; Clifford, S.; Ochterski, J.; Petersson, G. A.; Ayala, P. Y.; Cui, Q.; Morokuma, K.; Malick, D. K.; Rabuck, A. D.; Raghavachari, K.; Foresman, J. B.; Cioslowski, J.; Ortiz, J. V.; Stefanov, B. B.; Liu, G.; Liashenko, A.; Piskorz, P.; Komaromi, I.; Gomperts, R.; Martin, R. L.; Fox, D. J.; Keith, T.; Al-Laham, M. A.; Peng, C. Y.; Nanayakkara, A.; Gonzalez, C.; Challacombe, M.; Gill, P. M. W.; Johnson, B. G.; Chen, W.; Wong, M. W.; Andres, J. L.; Head-Gordon, M.; Replogle, E. S.; Pople, J. A. *Gaussian 98*, revision A.11.4; Gaussian, Inc.: Pittsburgh, PA, 1998.
(22) Chertihin, G. V.; Andrews, L. *J. Phys. Chem*. **1995**, *99*, 15004.
(23) Chertihin, G. V.; Andrews, L. *J. Am. Chem. Soc*. **1995**, *117*, 6402.
(24) Chatt, J.; Duncanson, L. A. *J. Chem. Soc*. **1953**, 2939.
(25) Dewar, M. J. S. *Bull. Soc. Chim. Fr*. **1951**, 79.
(26) Kushto, G. P.; Andrews, L. Unpublished work from this laboratory.